(18) W. C. Hamilton, *Acta Crystallogr.*, **18**, 502 (1965).
(19) The formula [Co(H₂O)₆][CoPhDTA] is assumed for the solid sample only because solution studies indicate the presence of the Co(H₂O)₆²⁺ ion; see text. Clearly a detailed study of crystals of the substance is required in order to definitively determine the nature of the coordination polyhedra.
(20) (a) M. A. Porai-Koshits, A. I. Pozhidaev, and T. N. Polynova, *Zh. Strukt. Khim.*, **15**, 1117 (1974). (b) For an interesting alternative method of classifying EDTA complexes see B. Lee, *Inorg. Chem.*, **11**, 1072 (1972).
(21) C. K. Johnson, "ORTEP", Report ORNL-3794, Oak Ridge National Laboratory, Oak Ridge, Tenn., 1965.
(22) At room temperature (21–25 °C) all the complexes exhibit magnetic moments per Co(II) ion of 4.6–4.9 μ_B. Thus, all can be considered high-spin complexes at room temperature.
(23) All "twist angles" mentioned are defined as the mean of the three twist angles formed using terminal atoms N(10)–N(20), O(11)–O(41), and O(21)–O(31) calculated using the centroids of the two triangles to define the twist-axis direction and the centroid of the six ligand atoms as the origin. For details see M. A. Flandera and E. C. Lingafelter, *Inorg. Chem.*, **15**, 750 (1976).
(24) T. N. Polynova, N. P. Bel'Skaya, D. Tyurk de Garciya Banos, M. A. Porai-Koshits, and L. I. Martynenko, *Zh. Strukt. Khim.*, **11**, 164 (1970).
(25) N. V. Novozhilova, T. N. Polynova, M. A. Porai-Koshits, N. I. Pechurova, L. I. Martynenko, and A. Khadi, *Zh. Strukt. Khim.*, **14**, 745 (1973).
(26) S. J. Rettig and J. Trotter, *Can. J. Chem.*, **51**, 1303 (1973).
(27) A. I. Pozhidaev, T. N. Polynova, M. A. Porai-Koshits, and N. N. Neronova, *Zh. Strukt. Khim.*, **14**, 570 (1973).
(28) N. V. Novozhilova, T. N. Polynova, M. A. Porai-Koshits, and L. I. Martynenko, *Zh. Strukt. Khim.*, **8**, 553 (1967).
(29) M. D. Lind, M. J. Hamor, T. A. Hamor, and J. L. Hoard, *Inorg. Chem.*, **3**, 34 (1964).
(30) Ya. M. Nesterova, T. N. Polynova, L. I. Martynenko, and N. I. Pechurova, *Zh. Strukt. Khim.*, **12**, 1110 (1971).
(31) A. I. Pozhidaev, T. N. Polynova, M. A. Porai-Koshits, and V. A. Logvinenko, *Zh. Strukt. Khim.*, **14**, 746 (1973).
(32) J. L. Hoard, B. Pedersen, S. Richards, and J. V. Silverton, *J. Am. Chem. Soc.*, **83**, 3533 (1961).

(33) T. M. Polynova, N. N. Anan'eva, M. A. Porai-Koshits, L. I. Martynenko, and N. I. Pechurova, *Zh. Strukt. Khim.*, **12**, 335 (1971).
(34) F. P. van Remoortere, J. J. Flynn, and F. P. Boer, *Inorg. Chem.*, **10**, 2313 (1971).
(35) G. H. Cohen and J. L. Hoard, *J. Am. Chem. Soc.*, **88**, 3228 (1966).
(36) In this work the conclusions about hexadentate (six- or seven-coordinate) EDTA⁴⁻ complexes do not include the Sn^II EDTA⁴⁻ complex reported by F. P. van Remoortere, J. J. Flynn, F. P. Boer, and P. P. North, *Inorg. Chem.*, **10**, 1511 (1971). Because one site in the coordination polyhedron is apparently occupied by a lone pair from the tin atom, this complex does not fit into either the hexadentate, six-coordinate or hexadentate, seven-coordinate classification.
(37) D. L. Kepert, *Inorg. Chem.*, **11**, 1561 (1972).
(38) The crystal-field calculations were performed in the manner of Companion and Komarynsky, *J. Chem. Educ.*, **41**, 257 (1964). The six donor atoms of PhDTA⁴⁻ were represented by 1– charges and the coordinates of the charges were computed as indicated in the text.
(39) W. C. E. Higginson and B. Samuel, *J. Chem. Soc. A*, 1579 (1970).
(40) T. R. Bhat and M. Krishnamurthy, *J. Inorg. Nucl. Chem.*, **25**, 1147 (1963).
(41) R. G. Wilkins and R. E. Yelin, *J. Am. Chem. Soc.*, **92**, 1191 (1970).
(42) J. A. Neal and N. J. Rose, *Inorg. Chem.*, **12**, 1226 (1973).
(43) K. Nakamoto, "Infrared Spectra of Inorganic and Coordination Compounds", Wiley, New York, N.Y., 1963.
(44) J. P. Hunt, Washington State University, Pullman, Wash., private communication.
(45) B. N. Figgis, "Introduction to Ligand Fields", Interscience, New York, N.Y., 1966.
(46) A. B. P. Lever, *Adv. Chem. Ser.*, No. 62, 430 (1967).
(47) W. C. E. Higginson, *J. Chem. Soc.*, 2761 (1962).
(48) R. A. Haines and B. E. Douglas, *Inorg. Chem.*, **4**, 452 (1965).
(49) G. S. Smith and J. L. Hoard, *J. Am. Chem. Soc.*, **81**, 556 (1959).
(50) G. D. Fallon and B. M. Gatehouse, *Acta Crystallogr., Sect. B.*, **30**, 1987 (1974).
(51) S. J. Lippard, H. Schugar, and C. Walling, *Inorg. Chem.*, **6**, 1825 (1967).
(52) A. B. P. Lever, "Inorganic Electronic Spectroscopy", Elsevier, New York, N.Y., 1968.

Crystal and Molecular Structures of *trans*-Tetrakis(pyridine)dichloroiron(II), -nickel(II), and -cobalt(II) and *trans*-Tetrakis(pyridine)dichloroiron(II) Monohydrate

GARY J. LONG* and PETER J. CLARKE

The crystal and molecular structures of Fe(py)₄Cl₂, Co(py)₄Cl₂, Ni(py)₄Cl₂, and Fe(py)₄Cl₂·H₂O have been determined from three-dimensional x-ray diffraction data collected on a four-circle diffractometer. The first three compounds crystallize in the tetragonal *I*4₁/*acd* space group with unit cell parameters of ca. 15.9 Å for *a* and ca. 17.1 Å for *b* and a volume of ca. 4350 Å³. Fe(py)₄Cl₂·H₂O crystallizes in the monoclinic *P*2₁/*c* space group with *a* = 9.384 (6) Å, *b* = 16.766 (4) Å, *c* = 16.342 (9) Å, *β* = 121.497 (25)°, and *V* = 2192.2 (1.2) Å.³ The structures were solved by Patterson and Fourier methods and refined where feasible by full-matrix least-squares procedures. All nonhydrogen atoms were refined with anisotropic thermal parameters and all pyridine hydrogen atoms were located by electron difference methods although more accurate positions were derived through geometric considerations; the resulting conventional *R* factors are 4.77, 4.83, 4.98, and 3.88%, respectively. In each complex the metal is coordinated in a trans fashion to two chloride ions and four pyridine molecules. The molecules, which possess 222 but not $\bar{4}$ symmetry, are oriented with their pseudotetragonal (Cl–M–Cl) axis normal to the tetragonal axis of the crystals. The individual molecules of M(py)₄Cl₂ are well isolated from each other with essentially no intermolecular contact distances of less than the sum of van der Waals radii. The one exception to this is Fe(py)₄Cl₂·H₂O where the water molecule serves as a presumably hydrogen-bonded bridge between two chloride ions in adjacent molecules. In the anhydrous iron, cobalt, and nickel complexes the M–Cl bond distances are 2.430 (3), 2.440 (2), and 2.437 (3) Å, and the M–N bond distances are 2.229 (6), 2.183 (4), and 2.133 (4) Å, respectively. The decrease in the M–N bond distance with increasing metal atomic number is attributed to the importance of the increasing number of t₂g π-bonding electrons in the metal ions. The relatively constant M–Cl bond distance is attributed to the constant number of σ-bonding electrons in these metal ions. The dihedral angle between the plane of the coordinate nitrogen atoms and the pyridine ring is ca. 51° in the anhydrous complexes. The increase of this dihedral angle above 45° is attributed either to a pyridine hydrogen to chlorine hydrogen-bonded interaction or to a hydrogen–carbon interaction on adjacent coordinated pyridine molecules.

Introduction

There have been many papers[1–8] which have dealt with the electronic and magnetic properties of tetrakis(pyridine)-

metal(II) chloride complexes. In several of these papers it has been assumed that the molecule possesses tetragonal symmetry with trans chloride ligands in the axial coordination positions and pyridine in the four equatorial positions. This is a reasonable assumption in view of the preliminary x-ray structural results for Ni(py)₄Cl₂—based on a two dimensional

*To whom correspondence should be addressed at the University of Missouri—Rolla.

Table I. Crystal Parameters and Intensity Data

	$Fe(py)_4Cl_2$	$Co(py)_4Cl_2$	$Ni(py)_4Cl_2^a$	$Fe(py)_4Cl_2 \cdot H_2O$
Formula	$FeC_{20}H_{20}N_4Cl_2$	$CoC_{20}H_{20}N_4Cl_2$	$NiC_{20}H_{20}N_4Cl_2$	$FeC_{20}H_{22}N_4OCl_2$
Mol wt	443.164	446.244	446.024	460.180
Crystal dimens, mm	0.80 × 0.36 × 0.18	1.02 × 0.23 × 0.18	0.89 × 0.30 × 0.18	0.86 × 0.23 × 0.16
Crystal class	Tetragonal	Tetragonal	Tetragonal	Monoclinic
Space group	$I4_1/acd$, No. 142, origin on $\bar{1}$	$I4_1/acd$, No. 142, origin on $\bar{1}$	$I4_1/acd$, No. 142, origin on $\bar{1}$	$P2_1/c$, No. 14
a, Å	15.945 (2)	15.966 (2)	15.920 (3)	9.384 (6)
b, Å				16.766 (4)
c, Å	17.287 (6)	17.153 (6)	17.046 (12)	16.342 (9)
β, deg				121.497 (25)
V, Å^3	4395.1 (2.7)	4372.5 (2.7)	4320.2 (4.8)	2192.2 (1.2)
Z	8	8	8	4
Calcd density, g cm^{-3}	1.340	1.356	1.372	1.394
Exptl density, g cm^{-3}	1.351 (1)	1.379 (1)	1.409 (1)	
Asymmetric unit	$Fe_{0.25}C_5H_5NCl_{0.5}$	$Co_{0.25}C_5H_5NCl_{0.5}$	$Ni_{0.25}C_5H_5NCl_{0.5}$	$FeC_{20}H_{20}N_4Cl_2H_2O$
Radiation	Mo Kα_1	Mo Kα_1	Mo Kα_1	Mo Kα_1
2θ limits, deg	0–60	0–60	0–60	0–50
Absorp coeff, cm^{-1}	9.6	10.7	11.6	9.7
Absorp cor	None	None	Empirical	None
Refined parameters	63	63	63	250
Reflections obsd	533	686	848	1798
Reflections unobsd	1133	914	730	1946
Unwtd R factor	4.77	4.83	4.98	3.88
Wtd R factor	6.52	6.68	7.48	4.53

^{a} Crystal used corresponded to $Ni_{0.97}Fe_{0.03}(py)_4Cl_2$ with 0.42 wt % Fe (see text).

refinement—obtained by Porai-Koshitz and Antsishkina[9] and the isomorphism exhibited by the iron, cobalt, and nickel complexes.[10] Unfortunately, although the early x-ray work indicated that the crystal class was tetragonal and of space group $I4_1/acd$, the results were not accurate enough to determine whether the molecule also possessed tetragonal symmetry. Because of our interest[11] in the magnetically perturbed single-crystal Mössbauer spectra of these compounds—doped with ^{57}Fe in the case of the cobalt and nickel complexes—we decided to determine the single-crystal x-ray structure of each of these salts. During the course of crystal preparation, a monohydrate of $Fe(py)_4Cl_2$ was also obtained and its crystal structure is reported herein. A further incentive for this work was our interest in the details of the metal–ligand bonding as a function of metal ion and the accompanying changes in the electronic structure of the metal ion.

In spite of the large number of studies on the electronic and magnetic properties of the various tetrakis(pyridine) complexes, there are relatively few complete x-ray structures reported. In addition to the above-mentioned structure, Porai-Koshitz and his co-workers[12] have also reported preliminary results on $Ni(py)_4Br_2$ and $Co(py)_4(NCS)_2$. More recently, Søtofte and Rasmussen have reported[13] the structure of $Fe(py)_4(NCS)_2$ and Hamm et al. have reported[14] on $Ni(py)_4I_2$. The situation is somewhat better for bis(pyridine) compounds. The important early work of Dunitz[15] on the pseudooctahedral polymeric $Co(py)_2Cl_2$ and $Cu(py)_2Cl_2$—pseudo-one-dimensional magnetic systems— has recently been refined and extended to the low-temperature γ form of $Co(py)_2Cl_2$ by Clarke and Milledge.[16] Richards et al. have also determined the structure[17] of $Mn(py)_2Cl_2$ and Morosin has refined and discussed[18] the structures of $Cu(py)_2Cl_2$ and $Cu(py)_2Br_2$, all of which possess the pseudooctahedral polymeric structure with bridging halide ligands. A study[19] of $Co(py)_2(NCS)_2$ revealed a polymeric octahedral structure with two equivalent nitrogen- and sulfur-bonded bridging thiocyanate ligands. A similar result[20] was found for $Cu(py)_2(NCS)_2$. In contrast, the structure of $Zn(py)_2Cl_2$ was recently reported[21] to contain a pseudotetrahedrally coordinated zinc ion. The only other type of pyridine complexes studied are $Co(py)_3(NO_3)_2$ and its analogous copper and zinc complex.[22] A comparison of the

relative metal–ligand bond distances in these complexes is used to relate the bonding to the nature of the electronic configuration of the metal.

Experimental Section

Preparation. Each of the compounds was prepared by adding a solution of the hydrated metal(II) chloride salt dissolved in methanol slowly to a solution of ca. 50% by volume of pyridine dissolved in methanol. The preparations of the iron compounds were carried out under a stream of nitrogen gas and with deoxygenated solvents to prevent oxidation of the iron(II). In each case the complex immediately precipitated and was removed by filtration after being stirred about 1 h. The mother liquor was then allowed to evaporate slowly producing single crystals of $M(py)_4Cl_2$. Evaporation of the mother liquor containing $Fe(py)_4Cl_2$ under nitrogen yielded anhydrous single crystals whereas evaporation in air yielded the monohydrate $Fe(py)_4Cl_2 \cdot H_2O$. Because the nickel complex was also prepared for single-crystal Mössbauer effect studies, these crystals were doped with 0.42 wt % of iron-57. All compounds gave satisfactory C, H, and N analyses.

Because the single crystals tend to lose pyridine from their surfaces, all crystals were immediately inserted, along with a small amount of mother liquor, into glass capillaries which were immediately sealed.

All experimental densities were measured by flotation in mixtures of 1,1-dichloroethane and 1,2-dibromoethane by using a Westphal balance.

Crystal Data. The approximate dimensions of the crystals used in this study are given in Table I.[23] The crystals were all mounted with their c axes approximately coincident with the spindle axis. Preliminary studies of the x-ray diffraction patterns were made by means of Weissenberg and precession methods, by using Ni-filtered Cu Kα and Zr-filtered Mo Kα radiations, respectively. The photographs obtained fit into two categories. The diffraction symmetry of the anhydrous compounds was $4/mmm$ and the systematic absences were hkl, $h = k = l = 2n + 1$; $hk0$, h $(k) = 2n + 1$; $0kl$, l $(k) = 2n + 1$; hkl $(l = 2n)$, $2h + 1 = 4n + 1$, indicating that the space group was $I4_1/acd$. The $Fe(py)_4Cl_2 \cdot H_2O$ crystals had diffraction symmetry $2/m$ and systematic absences $h0l$, $l = 2n + 1$; $0k0$, $k = 2n + 1$, indicating space group $P2_1/c$.

X-ray diffraction intensities were collected by means of a Hilger-Watts four-circle diffractometer with Mo Kα radiation (λ 0.710 69 Å) and a graphite monochromator (002). Unit cell parameters were determined by a least-squares method[24] from the positions of a number of automatically centered reflections. The parameters and their standard deviations are also given in Table I. Intensity data were collected by the ω–2θ scan technique with 50 steps of 0.02° in

Table II. Final Positional and Anisotropic Thermal ($\times 10^3$) Parameters for Nonhydrogen Atoms[a]

Atom	x	y	z	U_{11}	U_{22}	U_{33}	U_{12}	U_{13}	U_{23}
			$Fe(py)_4Cl_2$						
Fe	0.0000	0.2500	0.1250	48.3 (7)	48.3 (7)	39.1 (8)	0.2 (9)	0	0
Cl	0.1078 (1)	0.3578 (1)	0.1250	61 (1)	61 (1)	77 (2)	−13 (1)	−13 (1)	13 (1)
N	0.0716 (4)	0.1821 (4)	0.0337 (3)	64 (4)	50 (4)	48 (3)	6 (3)	9 (3)	7 (3)
C(1)	0.1098 (6)	0.2225 (6)	−0.0238 (4)	91 (7)	74 (5)	60 (4)	12 (5)	22 (5)	19 (4)
C(2)	0.1534 (7)	0.1818 (7)	−0.0821 (5)	99 (7)	101 (7)	74 (6)	34 (7)	48 (5)	23 (5)
C(3)	0.1597 (7)	0.0967 (7)	−0.0801 (5)	91 (7)	113 (8)	72 (6)	42 (6)	12 (5)	−12 (6)
C(4)	0.1194 (5)	0.0523 (6)	−0.0220 (5)	80 (6)	71 (5)	64 (5)	14 (5)	7 (5)	−6 (4)
C(5)	0.0767 (5)	0.0987 (5)	0.0328 (4)	64 (5)	53 (4)	59 (5)	−1 (4)	1 (4)	−2 (3)
			$Co(py)_4Cl_2$						
Co	0.0000	0.2500	0.1250	42.2 (4)	42.2 (4)	34.7 (5)	2.0 (7)	0	0
Cl	0.10826 (8)	0.35826 (8)	0.1250	55.3 (7)	55.3 (7)	68 (1)	−12.9 (8)	−9.6 (9)	9.6 (9)
N	0.0694 (3)	0.1828 (3)	0.0349 (2)	51 (3)	47 (3)	39 (2)	5 (2)	4 (2)	1 (2)
C(1)	0.1078 (4)	0.2229 (4)	−0.0227 (3)	70 (4)	64 (3)	51 (3)	9 (3)	22 (3)	17 (3)
C(2)	0.1524 (5)	0.1818 (5)	−0.0796 (4)	87 (5)	99 (5)	65 (4)	24 (4)	39 (4)	22 (4)
C(3)	0.1580 (5)	0.0964 (5)	−0.0773 (4)	86 (6)	94 (6)	68 (4)	31 (4)	18 (4)	−15 (4)
C(4)	0.1182 (4)	0.0547 (4)	−0.0195 (4)	76 (4)	61 (4)	63 (4)	20 (3)	2 (3)	−9 (3)
C(5)	0.0751 (4)	0.0995 (4)	0.0356 (3)	61 (3)	47 (3)	53 (3)	5 (3)	1 (3)	0 (3)
			$Ni(py)_4Cl_2$						
Ni	0.0000	0.2500	0.1250	38.4 (3)	38.4 (3)	32.5 (4)	1.5 (5)	0	0
Cl	0.10823 (7)	0.35823 (7)	0.1250	50.9 (5)	50.9 (5)	60.1 (9)	−10.4 (7)	−6.6 (7)	6.6 (7)
N	0.0677 (2)	0.1840 (2)	0.0363 (2)	48 (2)	43 (2)	38 (2)	3 (1)	3 (2)	1 (2)
C(1)	0.1065 (4)	0.2243 (3)	−0.0217 (3)	62 (3)	57 (3)	45 (2)	6 (2)	14 (2)	13 (2)
C(2)	0.1511 (4)	0.1829 (4)	−0.0786 (3)	75 (4)	80 (4)	57 (3)	19 (3)	28 (3)	17 (3)
C(3)	0.1567 (4)	0.0978 (5)	−0.0766 (3)	76 (4)	93 (5)	59 (3)	27 (3)	16 (3)	−11 (3)
C(4)	0.1174 (4)	0.0550 (3)	−0.0176 (3)	73 (4)	59 (3)	56 (3)	23 (3)	−1 (3)	−8 (2)
C(5)	0.0741 (3)	0.1004 (3)	0.0380 (3)	55 (3)	44 (2)	49 (2)	4 (2)	0 (2)	−1 (2)
			$Fe(py)_4Cl_2 \cdot H_2O$						
Fe	0.03888 (9)	0.24947 (5)	0.40401 (5)	44.4 (4)	46.7 (4)	52.2 (4)	0.5 (3)	26.1 (3)	−0.3 (4)
Cl(1)	0.2643 (2)	0.34545 (9)	0.4716 (1)	57.1 (9)	58.1 (9)	87 (1)	−11.4 (7)	35.4 (9)	−8.6 (8)
Cl(2)	−0.1905 (2)	0.15385 (9)	0.3419 (1)	57.8 (9)	62.0 (9)	84 (1)	−15.3 (7)	34.5 (8)	−10.7 (8)
N(1)	0.1631 (5)	0.1779 (3)	0.3414 (3)	47 (3)	63 (3)	53 (3)	7 (2)	25 (2)	3 (2)
C(11)	0.3283 (7)	0.1793 (4)	0.3803 (4)	55 (4)	79 (4)	66 (4)	2 (3)	32 (3)	0 (3)
C(12)	0.4079 (8)	0.1381 (4)	0.3423 (5)	71 (4)	108 (6)	92 (5)	23 (4)	56 (4)	8 (4)
C(13)	0.3161 (9)	0.0937 (4)	0.2621 (5)	105 (6)	103 (5)	84 (5)	46 (5)	63 (5)	14 (4)
C(14)	0.1473 (9)	0.0921 (5)	0.2210 (5)	95 (5)	112 (6)	58 (4)	21 (4)	34 (4)	−22 (4)
C(15)	0.0743 (7)	0.1343 (4)	0.2627 (4)	54 (4)	89 (5)	56 (4)	12 (3)	19 (3)	−13 (4)
N(2)	−0.0981 (5)	0.3214 (2)	0.4566 (3)	54 (3)	46 (3)	53 (3)	1 (2)	32 (2)	5 (2)
C(21)	−0.1184 (7)	0.3996 (3)	0.4408 (4)	61 (4)	52 (4)	60 (4)	4 (3)	33 (3)	4 (3)
C(22)	−0.2183 (7)	0.4458 (4)	0.4598 (4)	70 (4)	64 (4)	67 (4)	21 (3)	32 (4)	4 (3)
C(23)	−0.3022 (7)	0.4107 (4)	0.4988 (5)	67 (4)	88 (5)	76 (5)	20 (4)	41 (4)	−2 (4)
C(24)	−0.2808 (7)	0.3307 (4)	0.5177 (4)	70 (4)	89 (5)	75 (4)	−3 (3)	52 (4)	−4 (4)
C(25)	−0.1785 (7)	0.2879 (3)	0.4959 (4)	65 (4)	60 (3)	66 (4)	−4 (3)	39 (3)	1 (3)
N(3)	−0.0954 (5)	0.3196 (3)	0.2663 (3)	55 (3)	68 (3)	60 (3)	13 (2)	35 (3)	8 (2)
C(31)	−0.0142 (7)	0.3648 (4)	0.2365 (4)	67 (4)	108 (5)	74 (4)	21 (4)	49 (4)	25 (4)
C(32)	−0.0924 (9)	0.4123 (5)	0.1563 (5)	96 (6)	140 (7)	99 (6)	35 (5)	69 (5)	60 (5)
C(33)	−0.262 (1)	0.4146 (5)	0.1044 (5)	110 (6)	142 (7)	62 (4)	56 (5)	50 (4)	48 (5)
C(34)	−0.3480 (8)	0.3705 (5)	0.1329 (5)	69 (4)	126 (6)	59 (4)	34 (4)	28 (4)	20 (4)
C(35)	−0.2623 (7)	0.3229 (4)	0.2124 (4)	57 (4)	82 (4)	64 (4)	11 (3)	31 (3)	10 (4)
N(4)	0.1749 (5)	0.1777 (2)	0.5394 (3)	55 (3)	50 (3)	55 (3)	3 (2)	30 (2)	−5 (2)
C(41)	0.2611 (7)	0.2116 (4)	0.6260 (4)	73 (4)	70 (4)	58 (4)	7 (3)	36 (3)	−4 (3)
C(42)	0.3472 (8)	0.1682 (4)	0.7096 (4)	83 (5)	104 (6)	55 (4)	19 (4)	36 (4)	12 (4)
C(43)	0.3458 (8)	0.0867 (5)	0.7058 (5)	75 (5)	109 (6)	75 (5)	26 (4)	39 (4)	41 (5)
C(44)	0.2595 (8)	0.0512 (4)	0.6176 (5)	74 (4)	59 (4)	102 (5)	22 (3)	49 (4)	35 (4)
C(45)	0.1746 (8)	0.0975 (3)	0.5365 (4)	53 (3)	54 (4)	75 (4)	2 (3)	32 (3)	−5 (3)
O	0.5542 (8)	0.0679 (4)	0.1524 (5)	105 (3)[b]					

[a] The anisotropic temperature factors ($\times 10^3$) are of the form $\exp[-(h^2 a^{*2}U_{11} + k^2 b^{*2}U_{22} + l^2 c^{*2}U_{33} + 2hka^*b^*U_{12} + 2hla^*c^*U_{13} + 2klb^*c^*U_{2,j})]$. [b] Solvent oxygen refined isotropically only; occupancy factor for solvent H_2O is 0.76 (1).

ω. At least two equivalents of each reflection were measured for the tetragonal crystals but only one for the monoclinic case. Integrated intensities were extracted from the measured profiles via the ordinate-analysis approach[25] taking the 30 consecutive data points yielding the maximum gross intensity as the peak and the remaining 20 data points as the background. A scale factor of 1.5 was therefore necessary to relate the measured background to the gross peak intensity. Differential absorption curves[26] were measured for several reflections with χ setting angles close to 90°, but only in the case of $Ni(py)_4Cl_2$ was the absorption found to be large enough to warrant application of a correction. Data processing and structure refinement were carried out by using the "crystals" system computer program[27] and the Oxford University ICL 1906A computer. The Lorentz–polarization correction was applied to the measured intensities, and the data were merged

to yield sets of unique reflections. Intensities less than 4σ, where σ was the standard deviation from counting statistics, were classed as unobserved and rejected.

The structures were solved by Patterson and Fourier methods and refined where feasible by full-matrix least-squares calculations. For each structure, coordinates, scale factors, and isotropic temperature factors were refined until convergence, and hydrogen atoms were added in calculated positions. Further refinement of the scale factor and coordinates and anisotropic temperature factors for the nonhydrogen atoms yielded the final structural parameters given in Tables II and III. Final cycles for the monoclinic $Fe(py)_4Cl_2 \cdot H_2O$ structure, which had many more variable parameters than the others, were performed by using a block diagonal matrix approximation. The parameters were divided into seven blocks as follows: (1) all coordinates and the

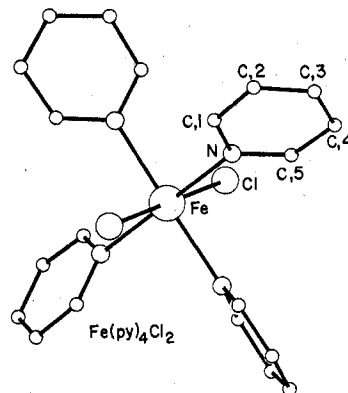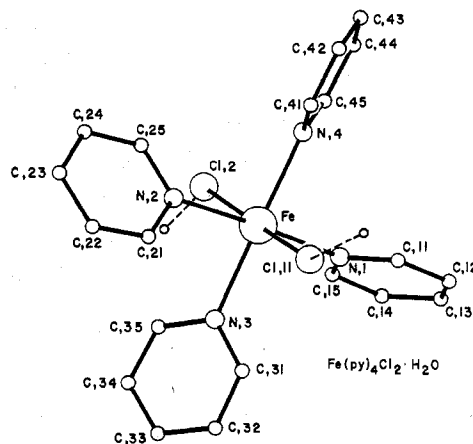**Table III.** Final Positional Parameters for Hydrogen Atoms

Atom	x	y	z
	$Fe(py)_4Cl_2$ ($U_{iso} = 0.090$ Å^2)		
H(1)	0.1086	0.2858	−0.0242
H(2)	0.1849	0.2139	−0.1246
H(3)	0.1915	0.0620	−0.1217
H(4)	0.1225	−0.0131	−0.0176
H(5)	0.0431	0.0659	0.0743
	$Co(py)_4Cl_2$ ($U_{iso} = 0.090$ Å^2)		
H(1)	0.1065	0.2865	−0.0229
H(2)	0.1817	0.2139	−0.1244
H(3)	0.1916	0.0624	−0.1189
H(4)	0.1220	−0.0115	−0.0143
H(5)	0.0430	0.0668	0.0774
	$Ni(py)_4Cl_2$ ($U_{iso} = 0.050$ Å^2)		
H(1)	0.1048	0.2876	−0.0222
H(2)	0.1796	0.2147	−0.1240
H(3)	0.1910	0.0637	−0.1181
H(4)	0.1219	−0.0106	−0.0122
H(5)	0.0429	0.0676	0.0802
	$Fe(py)_4Cl_2 \cdot H_2O$ ($U_{iso} = 0.050$ Å^2)		
H(11)	0.3977	0.2118	0.4399
H(12)	0.5327	0.1411	0.3741
H(13)	0.3712	0.0629	0.2338
H(14)	0.0766	0.0607	0.1609
H(15)	−0.0498	0.1316	0.2324
H(21)	−0.0563	0.4265	0.4138
H(22)	−0.2304	0.5044	0.4454
H(23)	−0.3769	0.4429	0.5128
H(24)	−0.3382	0.3034	0.5471
H(25)	−0.1639	0.2294	0.5100
H(31)	0.1109	0.3637	0.2747
H(32)	−0.0252	0.4443	0.1365
H(33)	−0.3208	0.4495	0.0462
H(34)	−0.4732	0.3721	0.0960
H(35)	−0.3280	0.2889	0.2314
H(41)	0.2629	0.2713	0.6302
H(42)	0.4109	0.1965	0.7728
H(43)	0.4065	0.0544	0.7662
H(44)	0.2583	−0.0083	0.6126
H(45)	0.1102	0.0702	0.4726

Figure 1. A perspective view of $Fe(py)_4Cl_2$ showing the molecular geometry and atomic numbering.

Figure 2. A perspective view of $Fe(py)_4Cl_2 \cdot H_2O$ showing the molecular geometry and atomic numbering.

isotropic temperature factor for the oxygen; (2) anisotropic temperature factors for Fe and Cl; (3) scale factors and dummy overall isotropic temperature factors; (4–7) anisotropic temperature factors for each of the four pyridine rings.

Atomic scattering factors were taken from ref 28, and anomalous dispersion corrections for respective metal and chlorine atoms were taken from ref 29. The function minimized was $\sum w(|F_o| - |F_c|)^2$. Initially, $w = 1$ for all data, but toward the end of the refinement values of w were calculated from a polynomial function based on a Chebyshev series.[30] The expression used for w was $w = 1/\sum_{n=0}^{n=l} A_n T_n^*(\chi)$, where n is the number of terms in the summation, A_n are the coefficients of the Chebyshev series, $T_n^*(\chi)$, and χ is $F_o/F_{o,max}$, where $F_{o,max}$ is the maximum value of the observed structure factor. The number of terms, n, and the coefficients, A_n, were determined such that $\sum w(|F_o| - |F_c|)^2$ was approximately unity for the complete data set and for various subsets of data systematically chosen

over ranges in $|F_o|$ and $(\sin \theta)/\lambda$. The values of A_n are given in Table IV.[31] The observed and calculated structure factors are presented in Table V.[31]

Results and Discussion

The results of the structural analysis indicate that the compounds have the expected trans chloride geometry with the pyridine nitrogen atoms approximately in a plane containing the metal ion (see below). The structure of the anhydrous $Fe(py)_4Cl_2$ molecule and the numbering scheme are shown in Figure 1. The structures of the cobalt and nickel complexes are essentially identical with that shown in Figure 1 and the same numbering scheme is used. The structure of the monohydrate, $Fe(py)_4Cl_2 \cdot H_2O$, is shown in Figure 2 along with the numbering scheme. The basic structure of this complex is quite similar to that of the anhydrous complex; however, the presence of the water molecule has lowered the symmetry of the crystal and the molecule making the four

Table VI. Intramolecular Bond Distances (Å)

	$Fe(py)_4Cl_2$	$Co(py)_4Cl_2$	$Ni(py)_4Cl_2$		$Fe(py)_4Cl_2$	$Co(py)_4Cl_2$	$Ni(py)_4Cl_2$
M–Cl	2.430 (3)	2.444 (2)	2.437 (2)	C(1)–C(2)	1.385 (12)	1.374 (9)	1.371 (8)
M–N	2.229 (6)	2.183 (4)	2.133 (4)	C(2)–C(3)	1.361 (13)	1.367 (10)	1.359 (9)
N–C(1)	1.331 (9)	1.329 (7)	1.330 (6)	C(3)–C(4)	1.386 (12)	1.352 (10)	1.366 (9)
N–C(5)	1.332 (9)	1.333 (7)	1.335 (6)	C(4)–C(5)	1.382 (10)	1.371 (8)	1.378 (7)
			$Fe(py)_4Cl_2 \cdot H_2O$				
Fe–Cl(1)	2.417 (2)	Fe–Cl(2)	2.440 (2)	Cl(1)–O	3.137 (7)	Cl(2)–O	3.107 (7)
Fe–N(1)	2.257 (4)	Fe–N(2)	2.236 (4)	Fe–N(3)	2.252 (4)	Fe–N(4)	2.241 (4)
N(1)–C(11)	1.333 (6)	N(2)–C(21)	1.331 (6)	N(3)–C(31)	1.335 (7)	N(4)–C(41)	1.335 (7)
N(1)–C(15)	1.328 (7)	N(2)–C(25)	1.342 (6)	N(3)–C(35)	1.338 (6)	N(4)–C(45)	1.346 (7)
C(11)–C(12)	1.382 (8)	C(21)–C(22)	1.371 (7)	C(31)–C(32)	1.373 (8)	C(41)–C(42)	1.377 (8)
C(12)–C(13)	1.354 (9)	C(22)–C(23)	1.377 (8)	C(32)–C(33)	1.354 (9)	C(42)–C(43)	1.367 (9)
C(13)–C(14)	1.359 (9)	C(23)–C(24)	1.368 (9)	C(33)–C(34)	1.348 (9)	C(43)–C(44)	1.367 (9)
C(14)–C(15)	1.386 (8)	C(24)–C(25)	1.386 (7)	C(34)–C(35)	1.371 (8)	C(44)–C(45)	1.376 (8)

Table VII. Bond Angles (deg)

	Fe(py)$_4$Cl$_2$	Co(py)$_4$Cl$_2$	Ni(py)$_4$Cl$_2$
Cl-M-N	88.92 (17)	89.35 (13)	89.49 (11)
	91.08 (17)	90.65 (13)	90.51 (11)
N-M-N	89.83 (29)	89.89 (20)	89.71 (19)
	90.21 (29)	90.12 (20)	90.30 (19)
	177.83 (33)	178.70 (20)	178.97 (21)
M-N-C(1)	121.9 (5)	121.6 (4)	121.6 (3)
M-N-C(5)	121.6 (5)	121.2 (4)	120.9 (3)
C(1)-N-C(5)	116.5 (7)	117.1 (5)	117.5 (4)
N-C(1)-C(2)	123.1 (9)	122.5 (6)	122.3 (5)
C(1)-C(2)-C(3)	119.0 (8)	119.4 (6)	119.8 (5)
C(2)-C(3)-C(4)	119.6 (8)	118.7 (6)	119.0 (5)
C(3)-C(4)-C(5)	116.8 (8)	119.0 (6)	118.3 (5)
C(4)-C(5)-N	124.9 (7)	123.3 (5)	123.1 (5)

	Fe(py)$_4$Cl$_2$·H$_2$O		
Cl(1)-Fe-Cl(2)	177.35 (6)	Cl(1)-O-Cl(2)	124.2 (2)
Cl(1)-Fe-N(1)	91.45 (12)	Cl(2)-Fe-N(1)	90.84 (12)
Cl(1)-Fe-N(2)	90.39 (11)	Cl(2)-Fe-N(2)	87.39 (11)
Cl(1)-Fe-N(3)	90.48 (13)	Cl(2)-Fe-N(3)	90.91 (12)
Cl(1)-Fe-N(4)	89.72 (12)	Cl(2)-Fe-N(4)	88.95 (12)
N(1)-Fe-N(3)	88.64 (15)		
N(1)-Fe-N(4)	89.98 (15)	N(1)-Fe-N(2)	176.37 (15)
N(2)-Fe-N(3)	88.22 (15)	N(3)-Fe-N(4)	178.61 (15)
N(2)-Fe-N(4)	93.15 (15)		
Fe-N(1)-C(11)	121.4 (4)	Fe-N(2)-C(21)	120.6 (3)
Fe-N(1)-C(15)	121.4 (3)	Fe-N(2)-C(25)	122.6 (4)
C(11)-N(1)-C(15)	117.2 (5)	C(21)-N(2)-C(25)	116.5 (5)
N(1)-C(11)-C(12)	123.0 (6)	N(2)-C(21)-C(22)	123.9 (5)
C(11)-C(12)-C(13)	119.3 (6)	C(21)-C(22)-C(23)	119.2 (5)
C(12)-C(13)-C(14)	118.5 (6)	C(22)-C(23)-C(24)	118.1 (5)
C(13)-C(14)-C(15)	119.6 (6)	C(23)-C(24)-C(25)	119.3 (5)
C(14)-C(15)-N(1)	122.4 (6)	C(24)-C(25)-N(2)	123.0 (5)
Fe-N(3)-C(31)	122.2 (4)	Fe-N(4)-C(41)	122.4 (4)
Fe-N(3)-C(35)	122.1 (4)	Fe-N(4)-C(45)	120.8 (4)
C(31)-N(3)-C(35)	115.6 (5)	C(41)-N(4)-C(45)	116.8 (5)
N(3)-C(31)-C(32)	123.7 (6)	N(4)-C(41)-C(42)	122.9 (6)
C(31)-C(32)-C(33)	118.8 (6)	C(41)-C(42)-C(43)	119.8 (6)
C(32)-C(33)-C(34)	119.2 (6)	C(42)-C(43)-C(44)	118.0 (6)
C(33)-C(34)-C(35)	119.0 (6)	C(43)-C(44)-C(45)	119.7 (6)
C(34)-C(35)-N(3)	123.6 (6)	C(44)-C(45)-N(4)	122.7 (6)
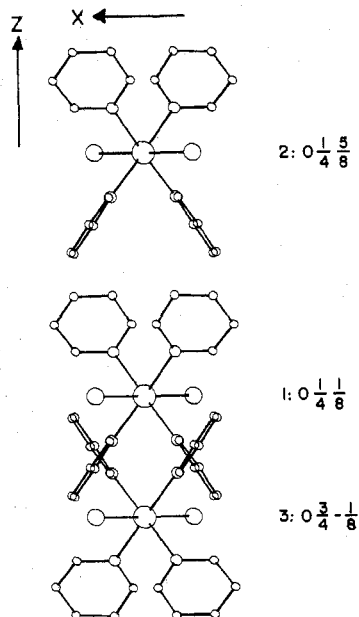
Figure 3. A perspective view of the orientations of molecules 1, 2, and 3 in the unit cell of Fe(py)$_4$Cl$_2$.

pyridine ligands crystallographically nonequivalent. The intramolecular bond distances in angstroms for each of the complexes are given in Table VI, and the intramolecular bond angles in degrees are given in Table VII. The equations for several least-squares planes through selected sets of atoms in the molecules are presented in Table VIII, along with the

Table VIII. Least-Squares Planes and Dihedral Angles

(a) Equations of Several Least-Squares Planes in the Form
$$Ax + By + Cz - D = 0$$

Compd	Plane	Atoms	A	B	C	D
Fe(py)$_4$Cl$_2$	1	FeN$_4$	11.275	11.275	0	2.819
	2	NC$_5$	−13.267	−0.891	−9.540	−1.426
Co(py)$_4$Cl$_2$	3	CoN$_4$	11.290	11.290	0	2.822
	4	NC$_5$	−13.187	−1.020	−9.607	−1.433
Ni(py)$_4$Cl$_2$	5	NiN$_4$	11.257	11.257	0	2.814
	6	NC$_5$	−13.167	−1.100	−9.509	−1.442
Fe(py)$_4$Cl$_2$·	7	FeN$_4$	6.036	11.142	−0.192	2.921
H$_2$O	8	N(1)C$_5$	−2.206	−13.308	9.823	0.626
	9	N(2)C$_5$	−3.335	−3.050	−9.741	−5.111
	10	N(3)C$_5$	3.113	−12.689	−10.680	−7.193
	11	N(4)C$_5$	9.361	0.367	−9.450	−3.395

(b) Atom Distances (Å) from Least-Squares Planes

Plane 1 Fe 0.000, N 0.042, N −0.042, N 0.042, N −0.042
Plane 2 N −0.008, C(1) −0.002, C(2) 0.013, C(3) −0.013,
  C(4) 0.005, C(5) 0.007, Fe 0.011, Cl 1.537, −1.515
Plane 3 Co 0.000, N 0.025, N −0.025, N 0.025, N −0.025
Plane 4 N −0.004, C(1) 0.003, C(2) 0.003, C(3) −0.007,
  C(4) 0.006, C(5) −0.001, Co −0.022, Cl 1.516, −1.561
Plane 5 Ni 0.000, N 0.019, N −0.019, N 0.019, N −0.019
Plane 6 N 0.004, C(1) −0.001, C(2) −0.001, C(3) 0.000,
  C(4) 0.003, C(5) −0.005, Ni −0.021, Cl 1.523, −1.565
Plane 7 Fe 0.016, N(1) −0.020, N(2) −0.020, N(3) 0.013,
  N(4) 0.012
Plane 8 N(1) 0.000, C(11) −0.001, C(12) −0.001, C(13) 0.005,
  C(14) −0.005, C(15) 0.003, Fe −0.063, Cl(1) −1.174,
  Cl(2) 1.106
Plane 9 N(2) 0.009, C(21) −0.008, C(22) 0.000, C(23) 0.006,
  C(24) −0.005, C(25) −0.003, Fe 0.284, Cl(1) −1.418,
  Cl(2) 1.946
Plane 10 N(4) −0.003, C(31) −0.005, C(32) 0.005, C(33) 0.003,
  C(34) −0.010, C(35) 0.010, Fe −0.166, Cl(1) −1.404,
  Cl(2) 0.996
Plane 11 N(4) 0.000, C(41) 0.001, C(42) 0.002, C(43) −0.006,
  C(44) 0.007, C(45) −0.005, Fe 0.033, Cl(1) 1.539,
  Cl(2) −1.563

(c) Dihedral Angles (deg) between Planes

1st plane	2nd plane	Angle	1st plane	2nd plane	Angle
1	2	51.11	8	9	106.64
3	4	51.01	8	10	78.06
5	6	50.68	8	11	106.83
7	8	62.27	9	10	57.58
7	9	45.72	9	11	107.28
7	10	59.75	10	11	69.39
7	11	50.90			

deviations of these atoms from the least-squares plane and the values for the dihedral angles contained in the molecule. Intramolecular contact distances, including chlorine to hydrogen contacts, but excluding all additional contacts with hydrogen, of less than 5.5 Å are listed in Table IX.[31]

Because of the unusual metamagnetic properties of the anhydrous complexes, it is of interest to study the details of the intermolecular interactions in these compounds. The eight crystallographically equivalent molecules in the unit cell yield four different types of relative orientation and hence four different sets of intermolecular contact distances (see Table IV). These involve the intermolecular contact of molecule 1 at 0, $^1/_4$, $^1/_8$ with molecule 2 at 0, $^1/_4$, $^5/_8$; with molecule 3 at 0, $^3/_4$, $-^1/_8$; with molecule 4 at $^1/_2$, $^1/_4$, $^3/_8$; and with molecule 5 at $^1/_2$, $^1/_4$, $-^1/_8$. Because it has proven extremely difficult to depict the contents of the entire unit cell with clarity, we have chosen to illustrate the intermolecular orientation in pairs. The relative orientation of molecules 1, 2, and 3 along c is illustrated in Figure 3. The relative orientation of molecules 1 and 2 along a and b is presented in Figure 4. Figures 5 and 6 show[31] the relative orientations of molecules 1, 4, and 5 and molecules 3, 4, and 5, respectively. The most interesting conclusion which may be reached by a
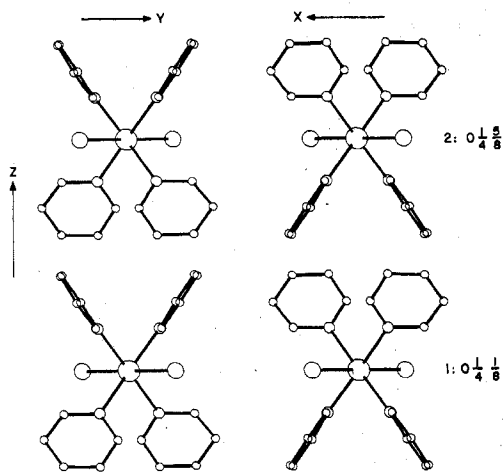
Figure 4. A perspective view of the orientations of molecules 1 and 2 in the unit cell of $Fe(py)_4Cl_2$.

study of Table IX and Figures 3–5 is that the individual molecules of $M(py)_4Cl_2$ are remarkably well isolated from each other. With the exception of hydrogen–hydrogen or hydrogen–pyridine carbon atom contacts, there are only ten intermolecular contact distances of less than 4.0 Å. Further, of these ten contacts, only three are less than 3.8 Å. Each of these three interactions occur between molecules 1 and 4 and involve contact with a chlorine atom (see Table IX). However, only the contact distance of ca. 2.8 Å between Cl, in molecule 1, and H(4), in molecule 4, is less than the sum of the van der Waals radii for the two involved atoms. Hence, it is not surprising that the iron, cobalt, and nickel complexes remain paramagnetic down to ca. 1.1 K in the absence of an applied field.[11] However, it seems rather unlikely that any through-bond intermolecular coupling could account for the magnetic properties observed for each of these compounds in an applied field.

The molecular structure of the $M(py)_4Cl_2$ molecule is the expected trans pseudooctahedral coordination geometry. A close study of the bonding about the metal ion reveals that the molecule does *not* possess the tetragonal symmetry as reported earlier by Porai-Koshitz and Antsishkina[9] for the nickel complex. The molecules possess 222 rather than $\bar{4}$ symmetry by virtue of the distortion of the Cl–M–N and N–M–N coordination bond angles from 90° and 180°, respectively (see Table VII). In each instance, the deviation of the Cl–M–N bond angle from 90° and the N–M–N bond angle from 180° is at least 5 times the standard error assigned to the bond angle and represents, we believe, a real deviation from tetragonal symmetry. The deviation from tetragonal symmetry is largest for the iron complex and smallest for the nickel complex. The Cl–Cl vector, the "pseudotetragonal" molecular axis, is *not* parallel with the crystallographic tetragonal axis. Rather, this vector is always normal to the crystallographic c axis and is alternately at plus or minus 45° to one of the crystallographic a axes (see molecules 1 and 2 in Figures 3 and 4). This has the unfortunate consequence of making it impossible to orient all the "pseudotetragonal" molecular axes in the crystal parallel with an external laboratory defined direction.

The metal–ligand bond distance in the three anhydrous tetrakis(pyridine) complexes provides a direct comparison of the variation of metal to chlorine and metal to pyridine bonding characteristics in these isomorphous compounds. In these compounds the metal to chlorine bond distances remain relatively constant. The largest difference in this bond length is 0.014 Å, the difference between the Fe–Cl bond distance of 2.430 (3) Å and the Co–Cl bond distance of 2.442 (2) Å. The difference, although probably real, is only ca. 3 times the

standard error in these bond distances. In contrast, the metal–pyridine bond distances differ by ca. 0.1 Å between the iron and nickel complexes. In comparison with the Fe–N bond distance of 2.229 (6) Å, the Co–N bond distance of 2.183 (4) Å is 0.046 Å shorter, and the Ni–N bond distance of 2.133 Å is 0.096 Å shorter. The differences are respectively ca. 5 and 10 times the standard error associated with these bond distances and are without question real differences.

The approximate constancy of the M–Cl bond distance relative to the variation of the M–N(pyridine) bond distance may be explained in terms of the mode of metal–ligand bonding. Adopting a simple crystal–ligand field model for the bonding in these pseudooctahedral complexes, it is noted that the iron, cobalt, and nickel complex ions have respectively the $t_{2g}^4 e_g^2$, $t_{2g}^5 e_g^2$, and $t_{2g}^6 e_g^2$ electronic configurations. In other words, the number of σ-bonding e_g electrons remains constant in the three compounds, while the number of π-bonding t_{2g} electrons increases from four to six. Because the chloride ion is bonded to the metal primarily via a σ-bonded interaction with the metal d_{z^2} orbital, it is not surprising that the metal–chlorine bond distance is relatively constant in these three complexes. In contrast the pyridine ligand is at least partly π bonded to the metal through an interaction with the metal t_{2g} orbitals. Hence, the nickel complex, with six π-bonding electrons, has a significantly shorter bond distance with pyridine than does the iron complex with only four π-bonding electrons. The parallel in the mean bond distance, 2.296, 2.269, and 2.234 Å for the iron, cobalt, and nickel complexes, respectively, and the ionic radii of the metal ions[32] results completely from changes in the metal–pyridine bond distance. In fact, the metal–chlorine bond distance trend is opposite to that expected from the ionic radii values. These bonding differences may also account for the parallel decrease in distortion of the molecules from $\bar{4}$ symmetry with increasing numbers of π-bonding electrons.

Reference to Table VIII(c) reveals that the dihedral angle between the least-squares MN_4 coordination plane and the least-squares plane of the pyridine molecule is ca. 51°, an angle which differs significantly from 45°. A significant electrostatic repulsion between chlorine and the pyridine H(1) and H(5) hydrogen atoms would tend to decrease this angle. Further, we believe, after a careful study of the molecular packing illustrated in Figures 3–6, that the optimum packing efficiency is obtained at a dihedral angle of 45°. This dihedral angle would be increased above 45° by (1) a significant Cl–H(1) hydrogen-bonding interaction, (2) a significant H(1)–H(5) electrostatic interaction between adjacent coordinated pyridine molecules, and (3) a significant H(1)–C(5) electrostatic interaction between adjacent coordinated pyridine molecules. Fisher–Hirschfelder–Taylor models indicate that the H(1)–C(5) interaction is more likely, and hence we conclude that either the H-bonded interaction or, more likely, the H(1)–C(5) interaction is most important in determining the final dihedral angle. Unfortunately, crystal packing effects cannot be completely eliminated.

The molecular structure of $Fe(py)_4Cl_2 \cdot H_2O$ is illustrated in Figure 2. The H_2O occupancy factor which was allowed to vary in the refinement process indicates only 0.76 occupancy. The oxygen atom is 3.107 (7) Å from Cl(2), located one unit cell along $+x$, and 3.137 (7) Å from Cl(1) obtained by the symmetry operator $(-x, -1/2 - y, -1/2 + z)$ and translated one unit cell along $-z$. The Cl(1)–O–Cl(2) angle is 124.2 (2)°. An attempt to locate the water hydrogen atoms by difference Fourier techniques was inconclusive but the Cl–O distance[33] for a chlorine atom hydrogen bonded to a water molecule is usually in the range 2.86–3.21 Å and we therefore conclude that the water molecule is hydrogen bonded, apparently in a rather symmetric fashion, to two chlorine atoms.

Table X. A Comparison of Several Structures Containing Pyridine

Metal	Compd	Ref	M–Cl, Å	Av M–Cl, Å	M–N, Å	Av M–N, Å
Mn	Mn(py)$_2$Cl$_2$	17	2.56, 2.57^a	2.565^a	2.24	2.24
Fe	Fe(py)$_4$Cl$_2$	b	2.430 (3)	2.430 (3)	2.229 (6)	2.229 (6)
Fe	Fe(py)$_4$Cl$_2$·H$_2$O	b	2.417 (2), 2.440 (2)	2.428 (2)	2.257 (4), 2.236 (4), 2.252 (4), 2.241 (4)	2.246 (4)
Fe	Fe(py)$_4$(NCS)$_2$	13			2.241 (4), 2.268 (4)	2.254 (4)
Co	Co(py)$_4$Cl$_2$	b	2.444 (2)	2.444 (2)	2.183 (4)	2.183 (4)
Co	α-Co(py)$_2$Cl$_2$	16	2.485 (7), 2.506 (7),^{a} 2.521 (7), 2.503 (7)	2.504 (7)^a	2.112 (16), 2.178 (16)	2.145 (16)
Co	γ-Co(py)$_2$Cl$_2$^{c}	16	2.435 (5), 2.507 (5)^a	2.471 (5)^a	2.156 (14)	2.156 (14)
Ni	Ni(py)$_4$Cl$_2$	b	2.437 (2)	2.437 (2)	2.133 (4)	2.133 (4)
Ni	Ni(py)$_4$I$_2$	14			2.114 (8), 2.130 (8)	2.124 (8)
Cu	Cu(py)$_2$Cl$_2$	18	2.299 (2), 3.026 (2)^a	2.662 (2)^a	2.004 (5)	2.004 (5)
Zn	Zn(py)$_2$Cl$_2$	21	2.215 (2), 2.228 (2)	2.222 (2)	2.046 (5), 2.052 (6)	2.049 (6)

^{a} For bridging chloride ions. ^{b} This work. ^{c} Structure at 89 K.

The major effect of the presence of the hydrogen-bonded water in Fe(py)$_4$Cl$_2$·H$_2$O is to reduce the symmetry of the unit cell and the molecule. Surprisingly, the additional H$_2$O molecule also reduces the volume of the unit cell. The volume for two unit cells of Fe(py)$_4$Cl$_2$·H$_2$O is 4384.4 Å^3, a reduction of 0.24% when compared with the 4395.1 Å^3 unit cell of Fe(py)$_4$Cl$_2$. The additional water molecule, although reducing the symmetry of the Fe(py)$_4$Cl$_2$ moiety relative to that in the anhydrous complex, has only a small effect on the coordination bond distances. The average Fe–Cl bond distance in the hydrate is the same (within experimental error) as the Fe–Cl distance in the anhydrous material. Further, the average Fe–N(pyridine) bond distance is only marginally (ca. 0.02 (1) Å) longer than in the anhydrate. The average coordination bond angle is also essentially the same in the hydrate as in the anhydrate. The geometry of the pyridine molecules is also essentially the same in the two forms of the complex. The major structural influence of the water molecule is observed in the four FeN$_4$–NC$_5$ dihedral angles. This angle ranges from 45.72 to 62.27°, with an average value of 54.7°. This range of dihedral angles, produced as a result of the water molecule, apparently provides enough flexibility within the Fe(py)$_4$Cl$_2$ moiety to improve the molecular packing and hence decrease the unit cell volume.

The structures of seven independent pyridine ligands are reported herein. Bond distances and angles are contained in Tables VI and VII. In all instances, the bond distances of the two equivalent bonds in a given pyridine molecule are found to agree within experimental limits. Likewise, with two exceptions, the bond angles at equivalent pyridine atoms in a given molecule are found to agree within experimental limits. In the two exceptions, the C(1)–C(2)–C(3) and C(3)–C(4)–C(5) bond angles in Fe(py)$_4$Cl$_2$ and Ni(py)$_4$Cl$_2$ agree to within 1.5σ.

The seven determinations of the pyridine ring structure under quite similar conditions permits a comparison of the details of the bonding in coordinated pyridine. A composite structure of pyridine, with the average equivalent bond distances and angles for all seven of the molecules, is presented in Figure 7. The values in parentheses in the figures are the standard deviations from the mean of the 7 or 14 values presented in Tables VI and VII. These average values indicate that the C(1)–C(2) bond distance is marginally longer than the C(3)–C(4) distance. The C(1)–C(2)–C(3) and C(2)–C(3)–C(4) average bond angles are equivalent to within experimental error. However, the N–C(1)–C(2) average bond angle is significantly greater than the other two carbon-centered angles. The C(1)–N–C(5) average bond angle is, as expected, significantly smaller than the carbon-centered angles. Similar results are found for most other coordinated pyridine molecules.[13–16,21,34]

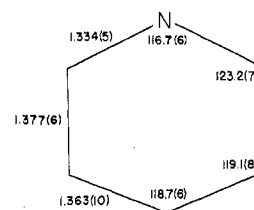The metal to chlorine and metal to pyridine nitrogen bond distances reported herein are compared with other recent

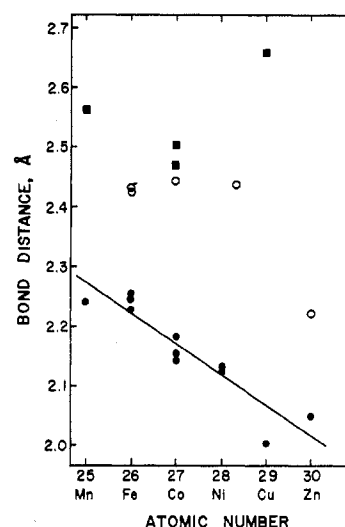**Figure 7.** The composite bond angles and distances for pyridine.

Figure 8. A plot of bond distance vs. metal atomic number for various pyridine complexes: ●, M–N distance; ○, M–Cl(terminal) distance; ■, M–Cl(bridge) average distance.

structural work on pyridine complexes in Table X and in Figure 8. The line in Figure 8 is a linear least-squares fit of the metal–pyridine nitrogen bond distance to the manganese to zinc atomic number and has a slope of −0.052 and an intercept of 2.273 Å at manganese. As discussed above, there is an obvious inverse relationship between the M–N(pyridine) bond distance and the atomic number of the metal, at least from manganese to zinc. This relationship is, no doubt, a combination of several factors. These include the increasing effective nuclear charge, the decreasing ionic radius, and increasing number of t$_{2g}$ π-bonding electrons, each of which change with increasing atomic number. It is interesting to note that on the basis of the slope in bond distances vs. atomic number for the pseudooctahedral manganese to copper complexes, the Zn–N bond distance would be ca. 2.01 Å. If the tetrahedral zinc complex is excluded from the slope calculation, a value of 1.99 Å is obtained. This short bond distance in a Zn(py)$_4$Cl$_2$-type complex would probably result in severe pyridine–pyridine interaction at H(1) and C(5) (see Figure 1). This may account for the formation of pseudo-

tetrahedral $Zn(py)_2Cl_2$ rather than $Zn(py)_4Cl_2$. There seems to be less of a systematic trend in the metal–chloride bond distances, partly as a result of both terminal and bridging chloride ions in these complexes. In general the bridging M–Cl bond distance is greater than the terminal M–Cl distance, a result not unexpected for three-centered bridging bonds. $Cu(py)_2Cl_2$, which contains the very asymmetric Cu–Cl bridging bond distances of 2.299 (2) and 3.026 (2) Å, has the largest average M–Cl bond distance whereas the pseudotetrahedral $Zn(py)_2Cl_2$ has the shortest M–Cl distance.

Registry No. $Fe(py)_4Cl_2$, 15245-99-5; $Co(py)_4Cl_2$, 14077-25-9; $Ni(py)_4Cl_2$, 14077-26-0; $Fe(py)_4Cl_2\cdot H_2O$, 65899-06-1.

Supplementary Material Available: Coefficients of the polynomial weighting scheme, Table IV, observed and calculated structure factors, Table V, intermolecular contact distances, Table IX, and perspective views of molecules 1, 4, and 5 and molecules 3, 4, and 5 in the unit cell of $Fe(py)_4Cl_2$, Figures 5 and 6 (72 pages). Ordering information is given on any current masthead page.

References and Notes

(1) G. J. Long, D. L. Whitney, and J. E. Kennedy, *Inorg. Chem.*, **10**, 1406 (1971).
(2) R. M. Golding, K. F. Mok, and J. F. Duncan, *Inorg. Chem.*, **5**, 774 (1966).
(3) C. D. Burbridge, D. M. L. Goodgame, and M. Goodgame, *J. Chem. Soc. A*, 349 (1967); D. M. L. Goodgame, M. Goodgame, M. A. Hitchman, and M. J. Weeks, *Inorg. Chem.*, **5**, 635 (1966); D. Forster and D. M. L. Goodgame, *ibid.*, **4**, 715 (1965).
(4) P. B. Merrithew, P. G. Rasmussen, and D. H. Vincent, *Inorg. Chem.*, **10**, 1401 (1971).
(5) M. Takeda, T. Tominaga, and N. Saito, *J. Inorg. Nucl. Chem.*, **36**, 2459 (1974).
(6) D. A. Rowley and R. S. Drago, *Inorg. Chem.*, **6**, 1092 (1967).
(7) W. M. Reiff, G. J. Long, and B. F. Little, *Inorg. Nucl. Chem. Lett.*, **12**, 405 (1976).
(8) M. Gerloch, R. F. McMeeking, and A. M. White, *J. Chem. Soc., Dalton Trans.*, 655 (1976).
(9) M. A. Porai-Koshitz and A. S. Antsishkina, *Tr. Inst. Kristallogr., Akad. Nauk SSSR*, **10**, 117 (1954).
(10) B. F. Little, Ph.D. Dissertation, University of Missouri—Rolla, 1978.
(11) G. J. Long and B. W. Dale, unpublished results.
(12) A. S. Antsishkina and M. A. Porai-Koshitz, *Sov. Phys.-Crystallogr. (Engl. Transl.)*, **3**, 684 (1960); M. A. Porai-Koshitz and G. N. Tishchenko, *Sov. Phys.-Crystallogr. (Engl. Transl.)*, **4**, 216 (1960).
(13) I. Søtofte and S. E. Rasmussen, *Acta Chem. Scand.*, **21**, 2028 (1967).
(14) D. J. Hamm, J. Bordner, and A. F. Schreiner, *Inorg. Chim. Acta*, **7**, 637 (1973).
(15) J. D. Dunitz, *Acta Crystallogr.*, **10**, 307 (1957).
(16) P. J. Clarke and H. J. Milledge, *Acta Crystallogr., Sect. B*, **31**, 1543, 1554 (1975).
(17) P. M. Richards, R. K. Quinn, and B. Morosin, *J. Chem. Phys.*, **59**, 4474 (1973).
(18) B. Morosin, *Acta Crystallogr., Sect. B*, **31**, 632 (1975).
(19) M. A. Porai-Koshitz and G. N. Tishchenko, *Kristallografiya*, **4**, 239 (1959); *Sov. Phys.-Crystallogr. (Engl. Transl.)*, **4**, 216 (1960).
(20) L. Macaskova, M. Kabesova, J. Garaj, and J. Gazo, *Monatsh. Chem.*, **104**, 1473 (1973).
(21) W. L. Steffen and G. J. Palenik, *Acta Crystallogr., Sect. B*, **32**, 298 (1976).
(22) A. F. Cameron, D. W. Taylor, and R. H. Nuttall, *J. Chem. Soc. A*, 3402 (1971).
(23) Numbers in parentheses here and elsewhere in this paper indicate estimated standard deviations in the least significant digits.
(24) M. Doebler and B. Duerr, personal communication.
(25) H. C. Watson, D. M. Shotton, J. M. Cox, and H. Muirhead, *Nature (London)*, **225**, 806 (1970).
(26) A. C. T. North, D. C. Phillips, and F. S. Mathews, *Acta Crystallogr., Sect. A*, **24**, 351 (1968).
(27) J. R. Carruthers and J. S. Rollett, personal communication.
(28) P. A. Doyle and J. M. Cowley in "International Tables for X-Ray Crystallography", Vol. 4, Kynoch Press, Birmingham, England, p 155, Table 2.4.6A.
(29) D. T. Cromer and J. A. Ibers in "International Tables for X-Ray Crystallography", Vol. 4, Kynoch Press, Birmingham, England, 1974, p 149, Table 2.3.1.
(30) J. S. Rollett, "Computing Methods in Crystallography", J. S. Rollett, Ed., Pergamon Press, New York, N.Y., 1965, p 40.
(31) Supplementary material.
(32) R. D. Shannon and C. T. Prewitt, *Acta Crystallogr., Sect. B*, **25**, 925 (1969); R. D. Shannon, *Acta Crystallogr., Sect. A*, **32**, 751 (1976).
(33) G. H. Stout and L. H. Jensen, "X-Ray Structure Determination", Macmillan, New York, N.Y., 1968, p 303.
(34) B. Salinas and E. O. Schlemper, personal communication.